Latent heat calculation of the three-dimensional $q=3$, 4, and 5 Potts models by the tensor product variational approach

A. Gendiar*
Institute of Electrical Engineering, Slovak Academy of Sciences, Dúbravská cesta 9, SK-842 39 Bratislava, Slovakia and Department of Physics, Faculty of Science, Kobe University, 657-8501, Japan

T. Nishino†
Department of Physics, Faculty of Science, Kobe University, 657-8501, Japan

(Received 23 February 2001; revised manuscript received 22 January 2002; published 10 April 2002)

Three-dimensional (3D) q-state Potts models ($q=3$, 4, and 5) are studied by the tensor product variational approach, which is a recently developed variational method for 3D classical lattice models. The variational state is given by a 2D product of local factors, and is improved by way of self-consistent calculations assisted by the corner transfer matrix renormalization group. It should be noted that no *a priori* condition is imposed for the local factor. Transition temperatures and latent heats are calculated from the observations of thermodynamic functions in both ordered and disordered phases.

DOI: 10.1103/PhysRevE.65.046702 PACS number(s): 02.70.−c, 75.10.Hk, 05.50.+q, 05.70.Fh

I. INTRODUCTION

The density matrix renormalization group (DMRG), which was invented by White in 1992 [1,2], has been applied to a wide class of one-dimensional (1D) quantum systems including quantum spin ladders [3]. DMRG is also efficient for obtaining thermodynamic functions of 2D classical systems [3,4]. Now a technical interest in DMRG is to extend its applicability to higher dimensional systems [5–7].

It is worth looking at the variational background in DMRG in order to obtain a rough image of DMRG in higher dimension. In 1995 Ostlund and Rommer showed that DMRG assumes so called ''the matrix product wave function,'' and that a very small numbers of parameters are sufficient to obtain a good variational energy [8]. It is a small surprise that such a construction of variational state has been known for long years in the field of statistical mechanics of 2D classical lattice models. In 1945 Kramers and Wannier introduced a very simple matrix product as a variational state for the transfer matrix of the 2D Ising model [9]. Later, the idea of constructing variational state from local elements was extended by Kikuchi [10] (the cluster approximation), Baxter [11,12], and Villani [13] (the correlation length equality approach). All these approaches calculate the lower bounds of the free energies of a 2D system. They use a variational state that corresponds to an effective 1D statistical system with several adjustable parameters.

Simply increasing the space dimension by one, we can extend such variational formula to three dimensions. The simplest example is the Kramers-Wannier approximation applied to the 3D Ising model by Okunishi and Nishino [14], where the 2D Ising model under the external magnetic field is treated as variational state, which has only two adjustable parameters. The calculated spontaneous magnetization and transition temperature are more precise than those obtained from a former attempt to extend DMRG to 3D classical systems [15]. A major problem in the Kramers-Wannier approximation is that one cannot always find out a good functional form of variational state intuitively, especially for models other than the 3D Ising model. In order to overcome this problem, a numerical self-consistent approach has been introduced, which we call the tensor product variational approach (TPVA) in the following [16,17]. In TPVA the variational state is determined automatically, with no reference to *a priori* information on systems. In this paper we briefly review the variational principle and the numerical algorithm of TPVA, and discuss the applicability of this method via trial calculations for $q=3$, 4, 5 Potts models.

In Sec. II we introduce main features of the algorithm from the variational point of view. We focus on the self-consistent improvement of the variational state. A specific way how to apply the variational method to the Potts model is presented in Sec. III. We also provide the way how to calculate the internal energy and the magnetization. The numerical results are presented in Sec. IV. In Sec. V we conclude the main results.

II. VARIATIONAL APPROACH IN TWO DIMENSIONS

For a tutorial purpose we first explain the way how to apply TPVA to the square lattice Potts model. (Later in the following section we treat the cubic lattice.)

Let us consider an infinitely long stripe of the width $2N$ on the square lattice, which is nothing but the $2N$-leg ladder, and consider the q-state Potts model in this finite width region. Figure 1 shows the transfer matrix $\mathcal{T}[\overline{\sigma}|\sigma]$ of this system when $2N=6$, where

$$[\sigma]=(\sigma_1,\sigma_2,\ldots,\sigma_{2N}) \quad \text{and} \quad [\overline{\sigma}]=(\overline{\sigma}_1,\overline{\sigma}_2,\ldots,\overline{\sigma}_{2N}) \tag{1}$$

represent adjacent rows of q-state spin variables. Here we interpret the Potts model as a special case of so called ''the

*Electronic address: gendiar@savba.sk
†Electronic address: nishino@phys.sci.kobe-u.ac.jp

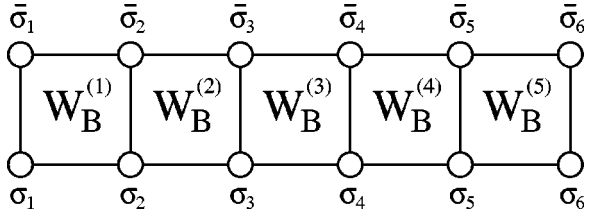

FIG. 1. The transfer matrix $\mathcal{T}[\bar{\sigma}|\sigma]$ in Eq. (2). This is the case where $2N=6$ and, therefore, there are five Boltzmann weights $W_B^{(i)}$ from $i=1$ to $i=5$.

interaction round a face'' (IRF) model [18], and construct $\mathcal{T}[\bar{\sigma}|\sigma]$ as a product of plaquette Boltzmann weights

$$\mathcal{T}[\bar{\sigma}|\sigma]=\prod_{i=1}^{2N-1} W_B(\bar{\sigma}_i\bar{\sigma}_{i+1}|\sigma_i\sigma_{i+1})=\prod_{i=1}^{2N-1} W_B^{(i)}\{\bar{\sigma}|\sigma\}, \tag{2}$$

where we have written the nearest neighbor spin pairs $(\sigma_i\sigma_{i+1})$ and $(\bar{\sigma}_i\bar{\sigma}_{i+1})$, respectively, as $\{\sigma\}$ and $\{\bar{\sigma}\}$ for the book keeping purpose. Following this index rule, the local Boltzmann weight is written as follows:

$$\begin{aligned} W_B^{(i)}\{\bar{\sigma}|\sigma\} &= W_B(\bar{\sigma}_i\bar{\sigma}_{i+1}|\sigma_i\sigma_{i+1}) \\ &= \exp\Bigg[-\frac{J}{2k_BT}(\delta_{\sigma_i\sigma_{i+1}}+\delta_{\bar{\sigma}_i\bar{\sigma}_{i+1}} \\ &\quad +\delta_{\sigma_i\bar{\sigma}_i}+\delta_{\sigma_{i+1}\bar{\sigma}_{i+1}})\Bigg], \end{aligned} \tag{3}$$

where we consider the ferromagnetic case $(J<0)$ throughout this paper.

The variational lower bound for the partition function per row is the maximum of the Rayleigh ratio

$$\lambda=\frac{\sum_{[\bar{\sigma}],[\sigma]}\Phi[\bar{\sigma}]\mathcal{T}[\bar{\sigma}|\sigma]\Psi[\sigma]}{\sum_{[\bar{\sigma}],[\sigma]}\Phi[\bar{\sigma}]\Psi[\sigma]}\equiv\frac{\langle\Phi|\mathcal{T}|\Psi\rangle}{\langle\Phi|\Psi\rangle}, \tag{4}$$

where $\Phi[\bar{\sigma}]$ and $\Phi[\sigma]$ are arbitrary variational states. Since the transfer matrix $\mathcal{T}$ in Eq. (2) is symmetric, we assume $\Phi[\sigma]=\Psi[\sigma]$ in the following.

TPVA consists of local approximations [16,17] that restrict the form of the variational state $\Psi[\sigma]$ into a uniform product of local factors

$$\Psi[\sigma]=\prod_{i=1}^{2N-1} V^{(i)}\{\sigma\}=\prod_{i=1}^{2N-1} V(\sigma_i\sigma_{i+1}), \tag{5}$$

where there are only q^2 variational parameters. Figure 2

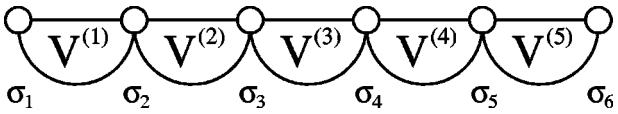

FIG. 2. Graphical expression of the variational state $\Psi[\sigma]$ in Eq. (5).

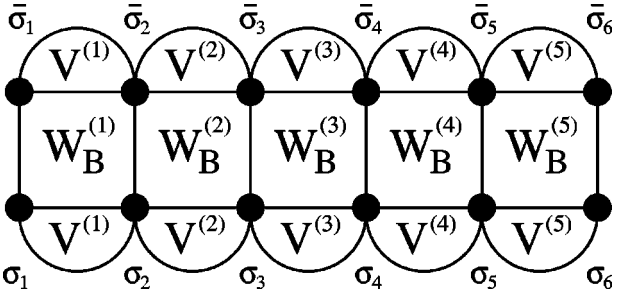

FIG. 3. Graphical expression of $\langle\Psi|\mathcal{T}|\Psi\rangle$ in Eq. (7). We have used black circles for the spins whose configuration sum is taken.

graphically represents $\Psi[\sigma]$ when $2N=6$. A profit of writing the variational state in the product form is that the norm of the variational state also has the local product structure

$$\langle\Psi|\Psi\rangle=\sum_{[\sigma]}\prod_{i=1}^{2N-1}[V^{(i)}\{\sigma\}]^2=\sum_{[\sigma]}\prod_{i=1}^{2N-1}[V(\sigma_i\sigma_{i+1})]^2, \tag{6}$$

which is nothing but a partition function of a 1D lattice model whose local Boltzmann weight is $[V(\sigma_i\sigma_{i+1})]^2$. In the same manner, the numerator of Eq. (4) is written as

$$\langle\Psi|\mathcal{T}|\Psi\rangle=\sum_{[\bar{\sigma}][\sigma]}\prod_{i=1}^{2N-1} V^{(i)}\{\bar{\sigma}\}W_B^{(i)}\{\bar{\sigma}|\sigma\}V^{(i)}\{\sigma\}, \tag{7}$$

which is also a partition function of an effective two-leg ladder. As we have graphically represented the variational state $\Psi[\sigma]$ in Fig. 2, let us also express $\langle\Psi|\mathcal{T}|\Psi\rangle$ graphically in Fig. 3.

With the use of the variational state thus defined, the variational problem in Eq. (4) is the same as those used by Villani [13,19]. Our aim is to obtain the best local factor $V\{\sigma\}$ numerically. There are several ways to maximize $\lambda_{\rm var}$ in Eq. (4), under the condition that the lattice size $2N$ is sufficiently large [16,17]. Keeping the extension to three dimensions in our mind, what we consider here is to take the variations of $\lambda_{\rm var}$ with respect to each local factor

$$\frac{\delta\lambda_{\rm var}}{\delta\Psi}\equiv\sum_i\frac{\delta\lambda_{\rm var}}{\delta V^{(i)}}. \tag{8}$$

When the system size $2N$ is large enough, it is sufficient to consider the variation with respect to the local change

$$V^{(N)}\to V^{(N)}+\delta V^{(N)} \tag{9}$$

at the center of the spin row, since we have treated the uniform variational state and since the boundary effect is negligible. After a short calculation from the (local) extremal condition [16,17]

$$\frac{\delta\lambda}{\delta V^{(N)}}=0, \tag{10}$$

we obtain an eigenvalue problem

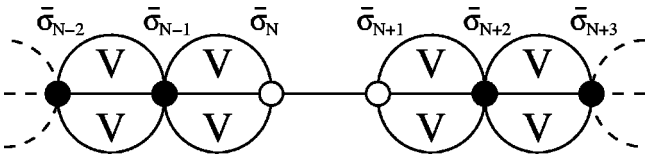

FIG. 4. The factor $A^{(N)}$ in Eq. (12) is constructed by joining two $\Psi[\sigma]$'s and taking spin configuration sum over all spins $[\sigma]$ (the black circles) except for the two central ones $\{\bar{\sigma}\}=(\bar{\sigma}_N,\bar{\sigma}_{N+1})$ (the white circles).

$$\sum_{\{\sigma\}} \frac{B^{(N)}\{\bar{\sigma}|\sigma\}}{A^{(N)}\{\bar{\sigma}\}} V^{(N)}\{\sigma\} = \lambda V^{(N)}\{\bar{\sigma}\} \tag{11}$$

for the local factor $V^{(N)}$. The new factor $A^{(N)}\{\bar{\sigma}\}$ is constructed as

$$A^{(N)}\{\bar{\sigma}\} = A\{\bar{\sigma}_N \bar{\sigma}_{N+1}\}$$

$$= \sum_{\bar{\sigma}_1 \ldots \bar{\sigma}_{N-1} \bar{\sigma}_{N+2} \ldots \bar{\sigma}_{2N}} \prod_{i \neq N} (V^{(i)}\{\bar{\sigma}\})^2, \tag{12}$$

whose graphical representation is shown in Fig. 4. The matrix $B^{(N)}$ is defined in the same manner

$$B^{(N)}\{\bar{\sigma}|\sigma\} = W_B^{(N)}\{\bar{\sigma}|\sigma\} \sum_{[\sigma][\sigma]}^{i \neq N, N+1} \prod_{i \neq N} V^{(i)}\{\bar{\sigma}\}$$

$$\times W_B^{(i)}\{\bar{\sigma}|\sigma\} V^{(i)}\{\sigma\}, \tag{13}$$

where the spin configuration sum is taken over all black circles in Fig. 5.

Since both $A^{(N)}$ and $B^{(N)}$ are constructed from the local factor V, the eigenvalue relation Eq. (11) should be solved self-consistently. Thus Eq. (11) is a kind of the self-consistent equation. A realistic outline how to solve the self-consistent equation is as follows.

(1) Start the calculation by setting (arbitrary) q^2 numbers of initial values for the local factor $V(\sigma,\sigma')$.

(2) Calculate $A^{(N)}$ and $B^{(N)}$ from Eqs. (12) and (13), respectively, for sufficient large system size $2N$.

(3) Substitute $A^{(N)}$, $B^{(N)}$, and $V^{(N)}$ to the left hand side of Eq. (11). Obtain the right hand side by

$$V'\{\bar{\sigma}\} = \sum_{\{\sigma\}} \frac{B^{(N)}\{\bar{\sigma}|\sigma\}}{A^{(N)}\{\bar{\sigma}\}} V^{(N)}\{\sigma\} \tag{14}$$

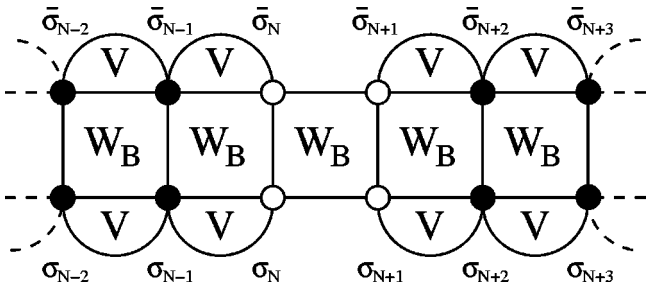

FIG. 5. Graphical representation of $B^{(N)}$ in Eq. (13).

and normalize it

$$V''\{\sigma\} = \frac{V'\{\sigma\}}{\sqrt{\sum_{\{\sigma'\}} (V'\{\sigma'\})^2}}. \tag{15}$$

(4) Create a linear combination $V_{\text{new}} = V + \varepsilon V''$ where ε is a small parameter of the order of 0.1, and regard it as an improved local factor. After normalizing V_{new} go to the second step and repeat the calculation till V reaches its (local) fixed point.

The small parameter ε is introduced in order to stabilize the convergence of the iterative calculation. For statistical models that exhibit a phase transition, the self-consistent equation has several stable solutions near the transition temperature. They correspond to the disordered state and to each ordered state. In such a case, one can ''target'' a desired phase just by imposing a very small symmetry-breaking field or by setting the initial local factor $V(\sigma,\sigma')$ appropriately.

The main advantage of the above algorithm is that no *a priori* ansatz is necessary for setting up the variational parameters.

III. EXTENSION TO THREE DIMENSIONS

It is easy to generalize both the variational relation [Eq. (4)] and the construction of the variational state in the product form [Eq. (5)] to 3D models. We can increase the space dimension by replacing the row-spin $[\sigma]$ in Eq. (1) to a ''layer spin''

$$[\sigma] = \begin{pmatrix} \sigma_{1\,1} & \cdots & \sigma_{1\,N} & \sigma_{1\,N+1} & \cdots & \sigma_{1\,2N} \\ \vdots & \ddots & \vdots & \vdots & \ddots & \vdots \\ \sigma_{N\,1} & \cdots & \sigma_{N\,N} & \sigma_{N\,N+1} & \cdots & \sigma_{N\,2N} \\ \sigma_{N+1\,1} & \cdots & \sigma_{N+1\,N} & \sigma_{N+1\,N+1} & \cdots & \sigma_{N+1\,2N} \\ \vdots & \ddots & \vdots & \vdots & \ddots & \vdots \\ \sigma_{2N\,1} & \cdots & \sigma_{2N\,N} & \sigma_{2N\,N+1} & \cdots & \sigma_{2N\,2N} \end{pmatrix}. \tag{16}$$

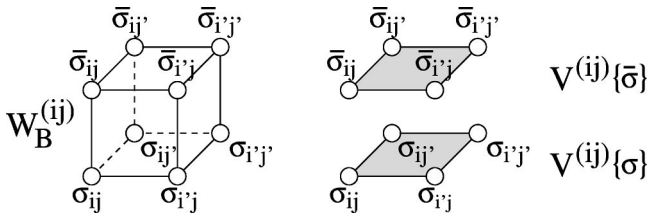

FIG. 6. The IRF-type local Boltzmann weight $W_B^{(ij)}\{\bar{\sigma}|\sigma\}$ of the q-state Potts models and the variational factors $V^{(ij)}\{\bar{\sigma}\}$ and $V^{(ij)}\{\sigma\}$. The q-state variables $\sigma=0,1,...,q-1$ are located at the edges of the cube. We use the notation $\{\bar{\sigma}\}$ and $\{\sigma\}$ for the upper and the lower horizontal plaquettes.

Now the system we are considering is an infinitely large 3D object of size $2N\times 2N\times\infty$. As before, we assume that the system size $2N$ is sufficiently large to investigate the bulk limit. The 3D generalization of the row-to-row transfer matrix in Eq. (2) is a layer-to-layer transfer matrix. For the 3D q-state Potts model, the layer-to-layer transfer matrix is given by

$$\mathcal{T}[\bar{\sigma}|\sigma]=\prod_{i=1}^{(2N-1)}\prod_{j=1}^{(2N-1)} W_B^{(ij)}\{\bar{\sigma}|\sigma\}, \tag{17}$$

where the IRF-type local Boltzmann weight is written as

$$\begin{aligned} W_B^{(ij)}\{\bar{\sigma}|\sigma\} &= W_B\begin{Bmatrix} \bar{\sigma}_{ij} & \bar{\sigma}_{i'j} & \bar{\sigma}_{i'j'} & \bar{\sigma}_{ij'} \\ \sigma_{ij} & \sigma_{i'j} & \sigma_{i'j'} & \sigma_{ij'} \end{Bmatrix} \\ &= \exp\Bigg[\frac{-J}{4k_BT}(\delta_{\sigma_{ij}\sigma_{i'j}}+\delta_{\sigma_{i'j}\sigma_{i'j'}}+\delta_{\sigma_{i'j'}\sigma_{ij'}} \\ &\quad +\delta_{\sigma_{ij'}\sigma_{ij}}+\delta_{\bar{\sigma}_{ij}\bar{\sigma}_{i'j}}+\delta_{\bar{\sigma}_{i'j}\bar{\sigma}_{i'j'}}+\delta_{\bar{\sigma}_{i'j'}\bar{\sigma}_{ij'}} \\ &\quad +\delta_{\bar{\sigma}_{ij'}\bar{\sigma}_{ij}}+\delta_{\sigma_{ij}\bar{\sigma}_{ij}}+\delta_{\sigma_{i'j}\bar{\sigma}_{i'j}}+\delta_{\sigma_{i'j'}\bar{\sigma}_{i'j'}} \\ &\quad +\delta_{\sigma_{ij'}\bar{\sigma}_{ij'}})\Bigg]. \end{aligned} \tag{18}$$

We have used the notation $i'=i+1$ and $j'=j+1$, and have represented the plaquette spins as $\{\sigma\}$. (See Fig. 6.)

The 2D generalization of the variational state in Eq. (5) can be obtained in the same manner,

$$\begin{aligned} \Psi[\sigma] &= \prod_{i=1}^{(2N-1)}\prod_{j=1}^{(2N-1)} V^{(ij)}\{\sigma\} \\ &= \prod_{i=1}^{(2N-1)}\prod_{j=1}^{(2N-1)} V(\sigma_{ij}\ \sigma_{i'j}\ \sigma_{i'j'}\ \sigma_{ij'}). \end{aligned} \tag{19}$$

There are q^4 variational parameters in the local factor $V^{(ij)}$. We assume that the factor $V^{(ij)}$ is positionally independent and the variational state is uniform. The local factor at the center of the system is $V^{(NN)}$.

The way how to optimize the local factor $V^{(ij)}$, so that it maximizes the Rayleigh ratio $\lambda_{\rm var}$ in Eq. (4), is, in principle, the same as that for 2D systems. The denominator

$$\langle\Psi|\Psi\rangle=\sum_{[\sigma]}\prod_{i=1}^{(2N-1)}\prod_{j=1}^{(2N-1)}(V^{(ij)}\{\sigma\})^2 \tag{20}$$

is nothing but a partition function of a 2D lattice model whose local Boltzmann weight is equal to $(V^{(ij)})^2$, and the numerator $\langle\Psi|\mathcal{T}|\Psi\rangle$ is that of a two-layer 2D lattice model

$$\sum_{[\sigma][\sigma]}\prod_{i=1}^{(2N-1)}\prod_{j=1}^{(2N-1)} V^{(ij)}\{\bar{\sigma}\}W_B^{(ij)}\{\bar{\sigma}|\sigma\}V^{(ij)}\{\sigma\}. \tag{21}$$

Since the numerator and the denominator are the partition functions of effective 2D lattice models one can calculate both of them using the corner transfer matrix renormalization group (CTMRG), which is a variant of DMRG applied to 2D lattice models [20]. As a byproduct of CTMRG, the factor $A^{(NN)}\{\sigma\}$ and the matrix $B^{(NN)}\{\bar{\sigma}|\sigma\}$ can be calculated [21]. Also, the variational free energy per site $\langle F\rangle$ can be obtained from CTMRG. (Numerical details are reported in Refs. [14,16,17].)

After we obtain the optimized variational factor $V^{(NN)}\{\sigma\}$, the internal energy E and the magnetization M can be calculated from $A^{(NN)}\{\sigma\}$ and $B^{(NN)}\{\bar{\sigma}|\sigma\}$ that are created from the optimized variational factor $V^{(NN)}$. The internal energy E per site is equivalent to

$$E=-J\delta(\sigma_{NN},\sigma_{N+1N})-J\delta(\sigma_{NN},\sigma_{NN+1})-J\delta(\sigma_{NN},\bar{\sigma}_{NN}) \tag{22}$$

and its statistical average is obtained as follows:

$$\langle E\rangle=\frac{\sum_{[\sigma][\sigma]}EV\{\bar{\sigma}\}B\{\bar{\sigma}|\sigma\}V\{\sigma\}}{\sum_{\{\sigma\}}V\{\sigma\}A\{\sigma\}V\{\sigma\}}, \tag{23}$$

where we have dropped the superscript (NN) from V, A, and B just for simplicity. The magnetization $\langle M\rangle$ of the q-state Potts model can be calculated from the spin expectation value

$$\langle\delta(\sigma,0)\rangle=\frac{\sum_{\{\sigma\}\{\sigma\}}\delta(\sigma_{NN},0)V\{\bar{\sigma}\}B\{\bar{\sigma}|\sigma\}V\{\sigma\}}{\sum_{\{\sigma\}}V\{\sigma\}A\{\sigma\}V\{\sigma\}} \tag{24}$$

together with the definition of the order parameter

$$\langle M\rangle=\frac{q\langle\delta(\sigma,0)\rangle-1}{q-1}. \tag{25}$$

IV. NUMERICAL RESULTS

We calculate the latent heat of the 3D $q=3$, 4, and 5 Potts models, using the internal energy expectation values $\langle E\rangle$ for both ordered and disordered phases. Hereafter we set $k_B=\mu_B=1$ and only treat the ferromagnetic case $J=-1$. The convergence control parameter in the self-consistent calculation is chosen as $\varepsilon=0.1$. When we obtain the variational state for the ordered phase, we impose a small symmetry-breaking field ($\sim$magnetic field) to the system during first

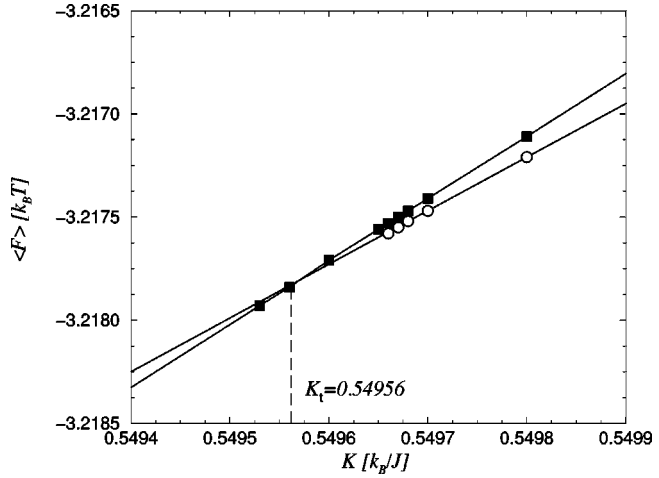

FIG. 7. The free energy per site $\langle F \rangle$ of the $q=3$ Potts model with respect to the inverse temperature $K=1/T$.

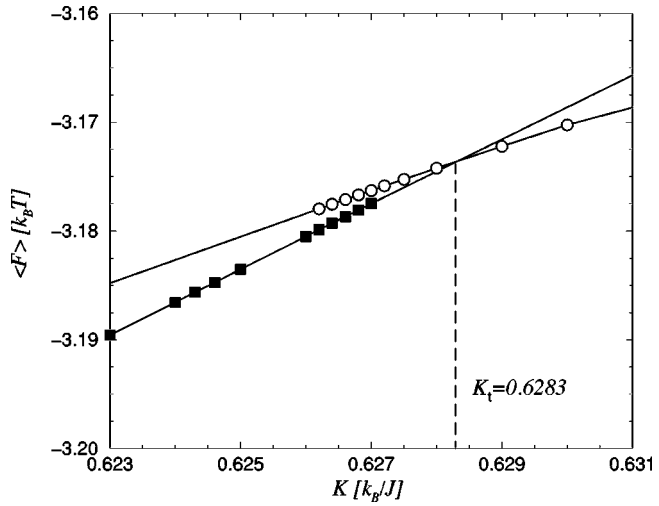

FIG. 8. The free energy per site $\langle F \rangle$ of the $q=4$ Potts model.

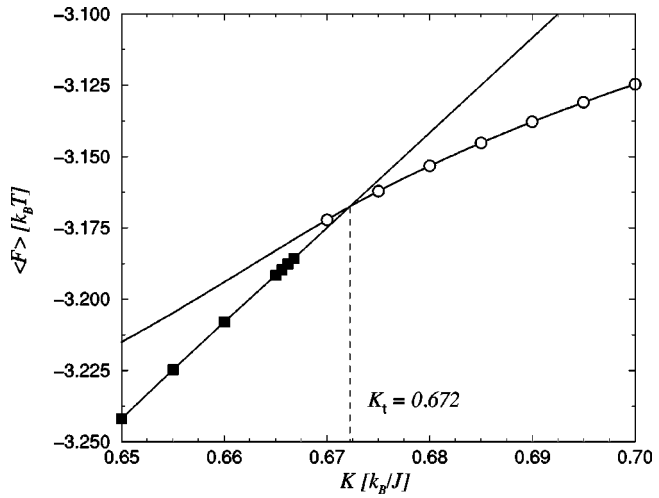

FIG. 9. The free energy per site $\langle F \rangle$ of the $q=5$ Potts model.

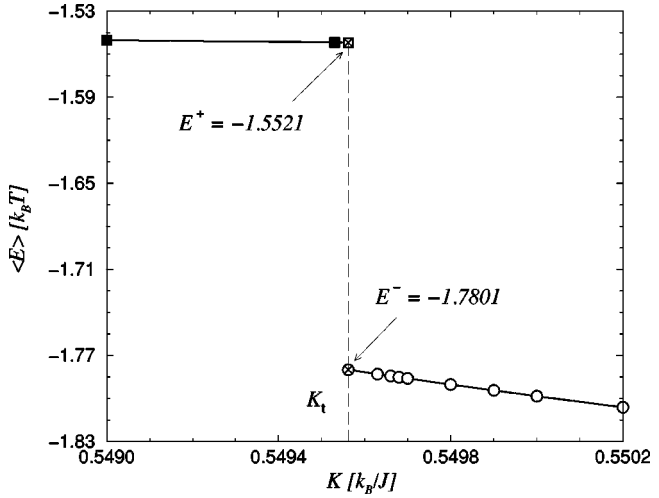

FIG. 10. The energy per site $\langle E \rangle$ with respect to K for the $q=3$ Potts model.

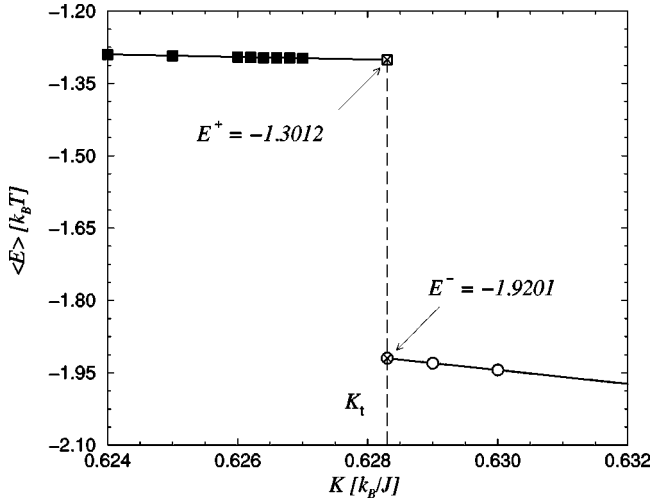

FIG. 11. The energy per site $\langle E \rangle$ with respect to K when $q=4$.

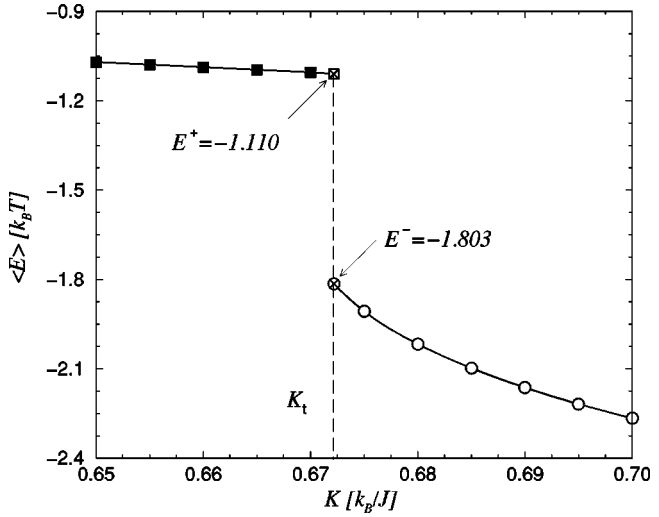

FIG. 12. The energy per site $\langle E \rangle$ with respect to K when $q=5$.

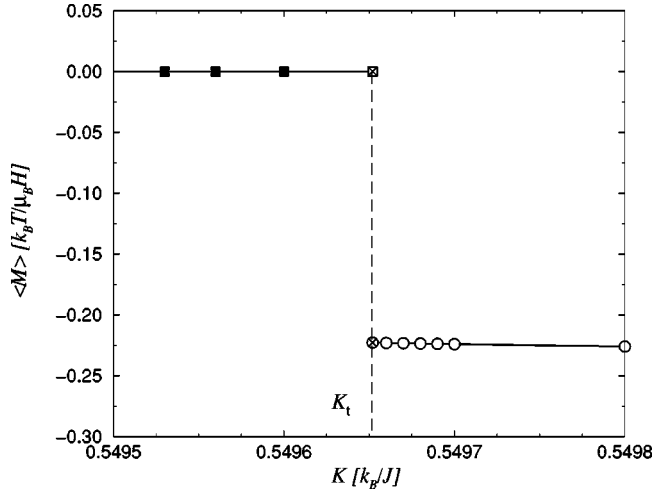

FIG. 13. The magnetization $\langle M\rangle$ with respect to the inverse temperature K for $q=3$.

several iterations, and after that we switch it off. For the CTMRG calculations, we kept block spin states m up to the value of 20 [22]; which is sufficiently large to obtain the thermodynamic functions shown below. All thermodynamic functions converged after 500 iterations at the most even in the close vicinity of the transition point.

First we determined the transition temperature from the calculated free energy per site $\langle F\rangle$ with respect to the inverse temperature $K\equiv 1/T$. Since the $q=3-5$ Potts models exhibit the first-order phase transitions, in a close vicinity of the transition point K_t there are two minima in the free energy F; one corresponds to the disordered phase and the other to the ordered one. It is possible to detect both of them by way of solving the self-consistent equation starting from different initial conditions for local factors. (When the barrier between the minima is low, one of the two phases is often accidentally chosen by numerical round-off errors.) Figures 7–9, respectively, show the calculated free energy per site $\langle F\rangle$ for $q=3$, 4, and 5 cases. The black squares and the white circles represent $\langle F\rangle$ for disordered and ordered phases, respectively,where the point of intersection of these two curves results the transition point K_t. The free energy curves were drawn by the least-square fitting of plotted data to polynomials. The results are, $K_t^{[q=3]}=0.5496$ for $q=3$, $K_t^{[q=4]}=0.6283$ for $q=4$, and $K_t^{[q=5]}=0.672$ for $q=5$. For the case $q=3$ the most reliable Monte Carlo (MC) result (as far as we know) is $K_t^{\mathrm{MC}}=0.550565\pm 0.000010$ [23], and thus $K_t^{[q=3]}$ calculated by TPVA is only 0.18% lower than K_t^{MC}.

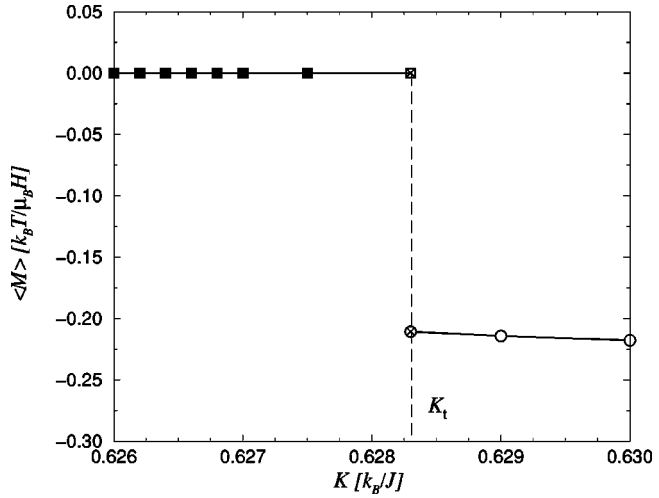

FIG. 14. The magnetization $\langle M\rangle$ with respect to K for $q=4$.

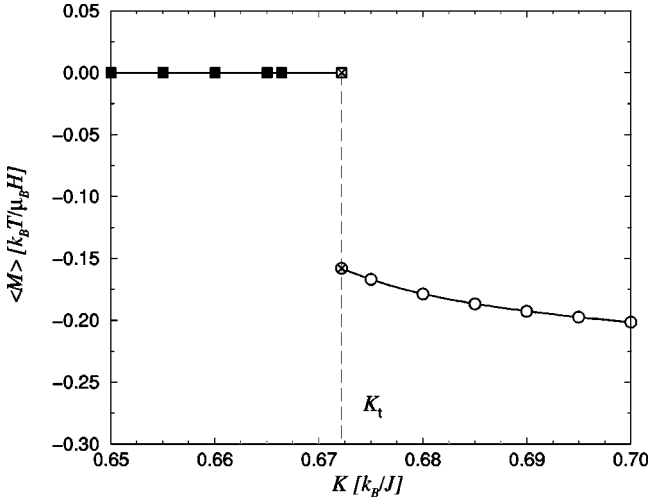

FIG. 15. The magnetization $\langle M\rangle$ with respect to K for $q=5$.

In Figs. 10–12, we have plotted the internal energies per site $\langle E\rangle$ as functions of $K\equiv 1/T$. The latent heat is the energy difference

$$Q=E^+-E^- \tag{26}$$

between the ordered and disordered phases. As before, we have applied the least-square fittings to interpolate (or extrapolate) the calculated data towards E^+ and E^- at the determined transition point $K_t^{[q=3,4,5]}$. These energies E^+ and E^-, respectively, are denoted by the cross symbols inside the squares and the circles in Figs. 10–12. The results are $Q^{[q=3]}=0.228$, $Q^{[q=4]}=0.619$, and $Q^{[q=5]}=0.693$. For the case $q=3$, $Q^{[q=3]}$ is 41% larger than a Monte Carlo result $Q_{\mathrm{MC}}^{[q=3]}=0.16160\pm 0.00047$ [23].

We finally show the calculated spontaneous

TABLE I. The numerically obtained transition points K_t and the latent heats Q by TPVA for the 3D ferromagnetic $q=3$, 4, and 5 state Potts models. The values of the m-state block spins are given in the second column.

q	m	K_t	Q
3	20	0.5496	0.228
4	20	0.6283	0.619
5	5	0.672	0.693

magnetization$\langle M \rangle$ in Figs. 13–15. All numerical results thus obtained are summarized in Table I.

V. CONCLUSIONS

Recently proposed self-consistent method for 3D classical systems, the TPVA, has been applied to $q=3$, 4, and 5 state Potts models on the simple cubic lattice. Thermodynamic functions such as the free energy, the internal energy, and the spontaneous magnetizations are calculated. The numerical algorithm for solving the self-consistent equation is stable at any temperature, if the convergence control parameter ε is chosen to be equal or smaller than 0.1.

ACKNOWLEDGMENTS

The authors thank Y. Hieida, K. Okunishi, N. Maeshima, and Y. Akutsu for discussions about variational formulations. This work has been partially supported by the Slovak Grant Agencies, VEGA No. 2/7201/21 and Grant-in-Aid for Scientific Research from Ministry of Education, Science, Sports and Culture (Grant No. 09640462 and No. 11640376). A.G. is supported by Japan Society for the Promotion of Science (P01192). The numerical calculations were performed by Compaq Fortran on the HPC-Alpha UP21264 Linux workstation.

[1] S. R. White, Phys. Rev. Lett. **69**, 2863 (1992).
[2] S. R. White, Phys. Rev. B **48**, 10 345 (1993).
[3] *Density-Matrix Renormalization—A New Numerical Method in Physics*, Lecture notes in Physics, edited by I. Peschel, X. Wang, M. Kaulke, and K. Hallberg, Vol. 528 (Springer Verlag, Berlin, 1999).
[4] T. Nishino, J. Phys. Soc. Jpn. **64**, 3598 (1995).
[5] S. D. Liang and H. B. Pang, Phys. Rev. B **49**, 9214 (1994).
[6] T. Xiang, J. Lou, and Z. B. Su, Phys. Rev. B **64**, 104414 (2001).
[7] M. C. Chung and I. Peschel, Phys. Rev. B **64**, 064412 (2001).
[8] S. Östlund and S. Rommer, Phys. Rev. Lett. **75**, 3537 (1995), S. Rommer and S. Östlund, Phys. Rev. B **55**, 2164 (1997).
[9] H. A. Kramers and G. H. Wannier, Phys. Rev. **60**, 263 (1941).
[10] R. Kikuchi, Phys. Rev. **81**, 988 (1951).
[11] R. Baxter, J. Math. Phys. **9**, 650 (1968); J. Stat. Phys. **19**, 461 (1978).
[12] R. J. Baxter and I. G. Enting, J. Stat. Phys. **21**, 103 (1979); R. J. Baxter, I. G. Enting, and S. K. Tsang, *ibid.* **22**, 465 (1980).
[13] M. Villani, J. Phys. A **23**, 4977 (1990); L. Angelini, M. Pellicoro, I. Sardella, and M. Villani, e-print cond-mat/9705062, and related papers.
[14] K. Okunishi and T. Nishino, Prog. Theor. Phys. **103**, 541 (2000).
[15] T. Nishino and K. Okunishi, J. Phys. Soc. Jpn. **68**, 3066 (1999).
[16] T. Nishino, K. Okunishi, Y. Hieida, N. Maeshima, and Y. Akutsu, Nucl. Phys. B **575**, 504 (2000).
[17] T. Nishino, K. Okunishi, Y. Hieida, N. Maeshima, Y. Akutsu, and A. Gendiar, Prog. Theor. Phys. **105**, 409 (2001).
[18] R. J. Baxter, *Exactly Solved Models in Statistical Mechanics* (Academic Press, London, 1982).
[19] Baxter used more general variational state, see Ref. [18].
[20] T. Nishino and K. Okunishi, J. Phys. Soc. Jpn. **65**, 891 (1996); **66**, 3040 (1997).
[21] One can calculate the factor $A^{(NN)}\{\sigma\}$ and the matrix $B^{(NN)}\{\overline{\sigma}|\sigma\}$ by combining the renormalized corner transfer matrix and the renormalized half-row transfer matrix.
[22] Both DMRG and CTMRG renormalizes a half-row spin into an m-state block spins. The CTMRG method yields equivalent results as DMRG in the thermodynamic limit for 2D classical lattice models.
[23] W. Janke and R. Villanova, Nucl. Phys. B **489**, 679 (1997).